


# First Human Trial of High-Frequency Irreversible Electroporation Therapy for Prostate Cancer

Technology in Cancer Research & Treatment  
Volume 17: 1-9  
© The Author(s) 2018  
Article reuse guidelines:  
sagepub.com/journals-permissions  
DOI: 10.1177/1533033818789692  
journals.sagepub.com/home/tct  


Shoulong Dong, PhD<sup>1</sup>, Haifeng Wang, PhD<sup>2</sup>, Yajun Zhao, BS<sup>1</sup>, Yinghao Sun, PhD<sup>2</sup>, and Chenguo Yao, PhD<sup>1</sup> 

## Abstract

Irreversible electroporation, as a nonthermal therapy of prostate cancer, has been used in clinic for several years. The mechanism of irreversible electroporation ablation is thermal independent; thus, the main structures (eg, rectum, urethra, and neurovascular bundle) in prostate are spared during the treatment, which leads to the retention of prostate function. However, various clinical trials have shown that muscle contractions occur during this therapy, which warrants deep muscle anesthesia. Use of high-frequency bipolar pulses has been proposed to reduce muscle contractions during treatment, which has already triggered a multitude of studies at the cellular and animal scale. In this study, we first investigated the efficacy and safety of high-frequency bipolar pulses in human prostate cancer ablation. There are 40 male patients with prostate cancer aged between 51 and 85 years involved in this study. All patients received 250 high-frequency bipolar pulse bursts with the repeat frequency of 1 Hz. Each burst comprised 20 individual pulses of 5 microseconds, so one burst total energized time was 100 microseconds. The number of the electrodes ranged 2 to 6, depending on tumor size. A small amount of muscle relaxant was still needed, so there were no visible muscle contractions during the pulse delivery process. Four weeks after treatment, it was found that the ablation margins were distinct in magnetic resonance imaging scans, and the prostate capsule and urethra were retained. Eight patients underwent radical prostatectomy for pathological analysis after treatment, and the results of hematoxylin and eosin staining revealed that the urethra and major vasculature in prostate have been preserved. By overlaying the electric field contour on the ablation zone, the electric field lethality threshold is determined to be  $522 \pm 74$  V/cm. This study is the first to validate the feasibility of tumor ablation by high-frequency bipolar pulses and provide valuable experience of irreversible electroporation in clinical applications.

## Keywords

irreversible electroporation, high-frequency bipolar pulses, prostate cancer, muscle contractions, cancer ablation

## Abbreviations

HF, high frequency; IRE, irreversible electroporation; MRI, magnetic resonance imaging; NVB, neurovascular bundle.

Received: December 31, 2017; Revised: April 10, 2018; Accepted: June 21, 2018.

## Introduction

Prostate cancer is one of the most common malignancies in men, and its morbidity significantly increases with age. Prostate cancer has the highest mortality rate among the cancers occurring in males, except for lung carcinoma in China.<sup>1</sup> There are many important structures proximal to the prostate, such as the rectum, urethra, and neurovascular bundle (NVB). Radical prostatectomy,<sup>2</sup> a conventional treatment technique for prostate cancer, wreaks havoc on the blood, NVB, and urethra, causing severe trauma and impotence. Newer minimally invasive

<sup>1</sup> State Key Laboratory of Power Transmission Equipment & System Security and New Technology, Chongqing University, Chongqing, People's Republic of China

<sup>2</sup> Department of Urology, Shanghai Changhai Hospital, Shanghai, People's Republic of China

### Corresponding Author:

Chenguo Yao, PhD, School of Electrical Engineering, Chongqing University, No. 174 Shazhengjie St., Shapingba Dist., Chongqing 400044, People's Republic of China.

Email: yaochenguo@cqu.edu.cn



**Table 1.** The Patients Treatment Information.

No	Number of Electrodes	Maximum Size of Tumor, cm	Number of Patients	Patients Age	Treatment Time, min
1	2	<1	3	64, 76, 79	<8
2	3	1.0-1.5	13	81, 71, 59, 71, 82, 74, 69, 59, 79, 67, 51, 58, 63	<20
3	4	1.5-2.0	10	76, 68, 73, 57, 65, 81, 84, 85, 73, 78	<30
4	5	2.0-2.5	8	68, 51, 65, 74, 68, 76, 82, 75	<40
5	6	2.5-3.0	6	75, 66, 75, 64, 72, 77	<45

thermal-based therapies, including cryoablation,<sup>3</sup> radiofrequency ablation,<sup>4,5</sup> and microwave ablation, ablate the tumor when the temperature is higher or lower than a critical value. However, the ablation of tumors near blood vessels is affected because of the heat-sink effect. Another limitation of these thermal-based therapies is that they are nonselective because the aforementioned proximal structures can be damaged, leading to some complications.

Irreversible electroporation (IRE) is a new nonthermal ablation modality that employs intensive and narrow electric pulses to create permanent defects on the cell membrane, resulting in cell death.<sup>6,7</sup> Contrast to thermal therapies, the mechanism of IRE is thermal independent, making it possible to ablate the tumors near the heat-sensitive structures. Optimization of pulse parameters and the arrangement of electrodes allow the vessels and nerves to be spared during treatment, which is beneficial for the patients' recovery and retaining prostate function. Additionally, the ablation results of IRE remain unaffected by blood perfusion because of its nonthermal mechanism.<sup>8,9</sup> These characteristics enable the wide application of IRE in clinics. Following the first clinical trial of IRE on prostate cancer treatment, IRE has been found to be useful in various clinical applications.<sup>10-13</sup>

Typically, IRE utilizes 80 to 120 unipolar pulses applied for a duration of 50 to 100 microseconds and at a voltage-to-distance ratio of >1000 V/cm. The pulses are delivered in synchrony with the patient's heartbeat to minimize adverse cardiac events or at a frequency of 0.1 to 5 Hz.<sup>14-16</sup> However, this protocol can evoke muscle contractions during the pulse delivery process, which may cause pain to the patients and bring about a displacement of the electrodes, thereby adversely affecting the ablation outcome.<sup>9,17</sup> Therefore, a deep neuromuscular blockade is necessary to ensure that the IRE treatment goes smoothly.

Arena *et al*<sup>18</sup> proposed a new-generation IRE technique to mitigate the impact of muscle contractions, namely, high-frequency IRE (also called as H-FIRE). This new type of pulse consists of a set of bipolar pulse bursts, and each burst comprises a number of individual pulses of duration ranging between 0.5 and 10 microseconds, and the total energized time of each burst is in the order of 100 microseconds. Some experiments involving the use of HF bipolar pulses have previously been conducted on cells and animals to verify the efficacy of HF bipolar pulses on the tumor-killing effect and reduction in muscle contraction.<sup>19,20</sup> The studies showed that the muscle

contraction inhibition and tissue ablation characteristics are closely related to the duration of individual HF bipolar pulses.

Although several studies have been conducted regarding the effects of HF bipolar pulses on cells and tissues and there is strong evidence that such pulses can be used for tumor therapy, the efficacy and safety of their clinical application have not yet been studied. Our group has developed a tumor therapy apparatus that can generate both regular IRE pulses and HF bipolar pulses, and it has passed the registration test at the Shanghai Testing and Inspection Institute for Medical Devices. This article details the first human trial of HF bipolar pulses for treating prostate cancer using the apparatus developed by our group, and magnetic resonance imaging (MRI) and ultrasound were combined to locate the tumor in the prostate and guide electrode insertion during treatment. Four weeks after the treatment, MRI was used to image the ablation zone and the prostate was resected for pathological examination. The electric field threshold of ablation could be determined by overlaying the electric field contours on the ablation zone. This clinical trial validated the feasibility of the clinical use of HF bipolar pulses for prostate cancer treatment, thereby promoting various clinical applications of our technique.

## Methods

### Patient Information

Clinical trials were performed after obtaining patients' consent and approval from the Shanghai Changhai Hospital Ethics Committee (CHEC2017-075) and Good Clinical Practices. Forty patients received therapeutic HF bipolar pulses, and their ages were in the range 51 to 85 years. The patients were treated at Shanghai Changhai Hospital in Shanghai, China. Significantly elevated prostate-specific antigen level was detected in patients, and the patients then underwent multiparametric MRI to detect the suspected tumor in their prostate; the maximum tumor size in all patients was 1 to 3 cm. The patients' treatment information is listed in Table 1. A needle biopsy was performed before the IRE procedure to demonstrate the clinical significance of prostate cancer through histological analysis.

### Therapeutic Equipment

A composite steep pulse therapeutic apparatus was used to generate HF bipolar pulses, as shown in Figure 1A. The apparatus can produce bursts of HF bipolar pulses, constituting of

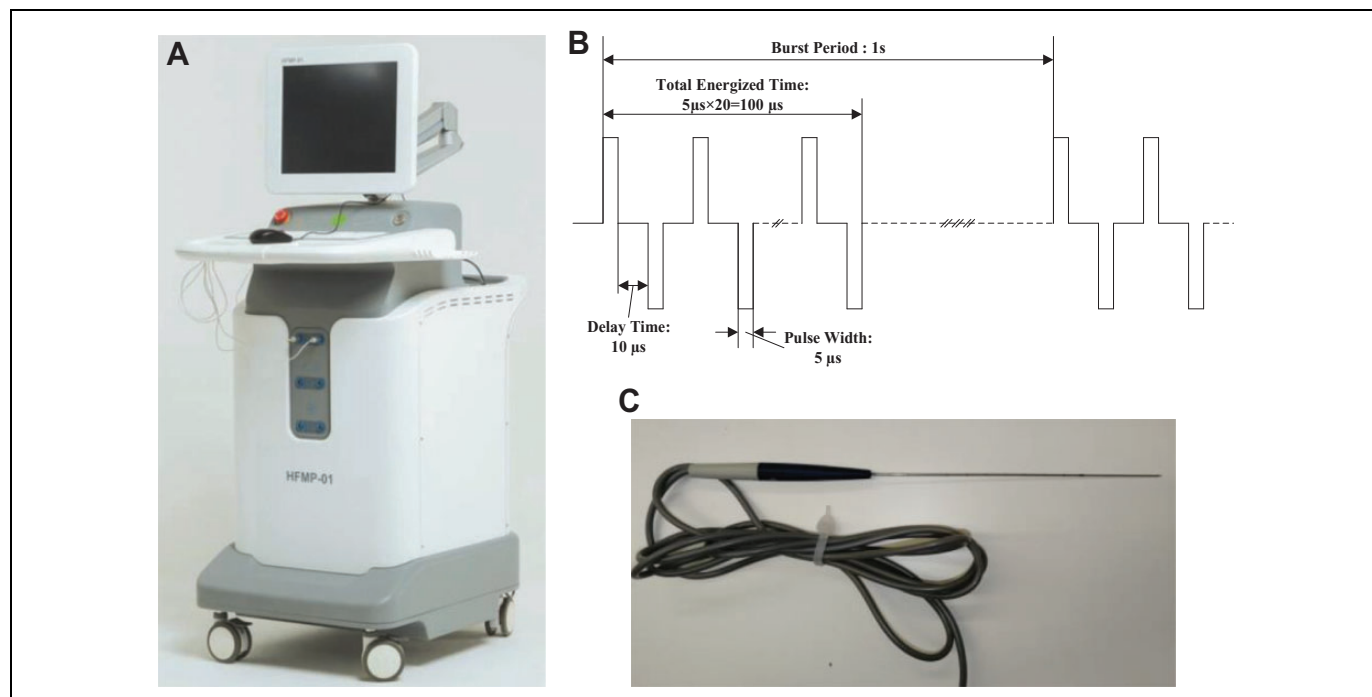


**Figure 1.** The picture of (A) composite steep pulse therapeutic apparatus and (B) the schematic of HF bipolar pulses. (C) Electrodes. HF indicates high frequency.

individual pulses of duration ranging from 1 to 100 microseconds; the interburst delay is 1 second, and the rise time is less than 100 nanoseconds. The schematic of bipolar HF pulse bursts applied in this study is shown in Figure 1B.

In each trial, 2 to 6 needle electrodes were inserted into the tumor region, and the distance between 2 electrodes was  $<2$  cm. The diameter of the electrodes was 1 mm, and the exposure length was set to 1.0 to 3.0 cm (Figure 1B), depending on the tumor's size.

### Procedure

The patients were placed in the dorsal lithotomy position and were operated under aseptic conditions and general anesthesia. In order to administer a lower concentration of muscle relaxant to patients, a muscle relaxant (cisatracurium besylate) at a dose of only 0.001 mg/kg·min was injected, which was lower than the dose used during a conventional surgery (0.0015 mg/kg·min).<sup>21</sup>

Then, the therapeutic electrodes were punctured transperineally at the margin of the cancer lesion under transrectal ultrasound guidance, and the space between electrodes was measured using ultrasound images.

High-frequency bipolar pulses were delivered after the position of the needle electrodes was determined. The burst of HF bipolar pulses, consisting of 20 pulses each of 5 microseconds, had a total energized time of 100 microseconds, with a 10- $\mu$ s delay time between the positive and the negative pulses. The schematic of HF bipolar pulses is given in Figure 1C. The initial voltage-to-distance ratio applied was 1500 V/cm between the pairs of electrodes. The voltage was adjusted

during the trial to avoid a very large pulse current ( $>40$  A). Pulses were delivered at a repetition rate of 1 burst/second in sets of 50 pulses, following a 10-second delay to avoid an increase in temperature in the tissues; this cycle was repeated for a total number of 250 bursts that were delivered between each pair of electrodes. The electrodes were removed after treatment, and the patient was inserted with a urethral catheter and left to wake up.

### Therapeutic Effect Evaluation

Four weeks after treatment, MRI was used to estimate the ablation area. In addition, the position of the electrodes in MRI image, which would be used to analyze the electric field threshold of ablation, was determined by matching the MRI image and the ultrasound image with the location of electrodes.

The efficacy of ablation at the cellular level was analyzed in 8 patients who underwent complete resection of the prostate after 4 weeks based on voluntary principles. These prostates were sectioned and processed for histology analysis using hematoxylin and eosin staining. Color images of each tissue section were acquired using the Aperio LV1 Digital Pathology Slide Scanner (Leica Biosystems Inc, Buffalo Grove, Illinois).

### Numerical Simulations

It was difficult to reconstruct an accurate 3D model because only low-resolution MRI slices were acquired. Therefore, a 2D finite element model of the prostate tissue was established using COMSOL Multiphysics software (version 4.2a; COMSOL Inc, Burlington, Massachusetts). As shown in Figure 2,

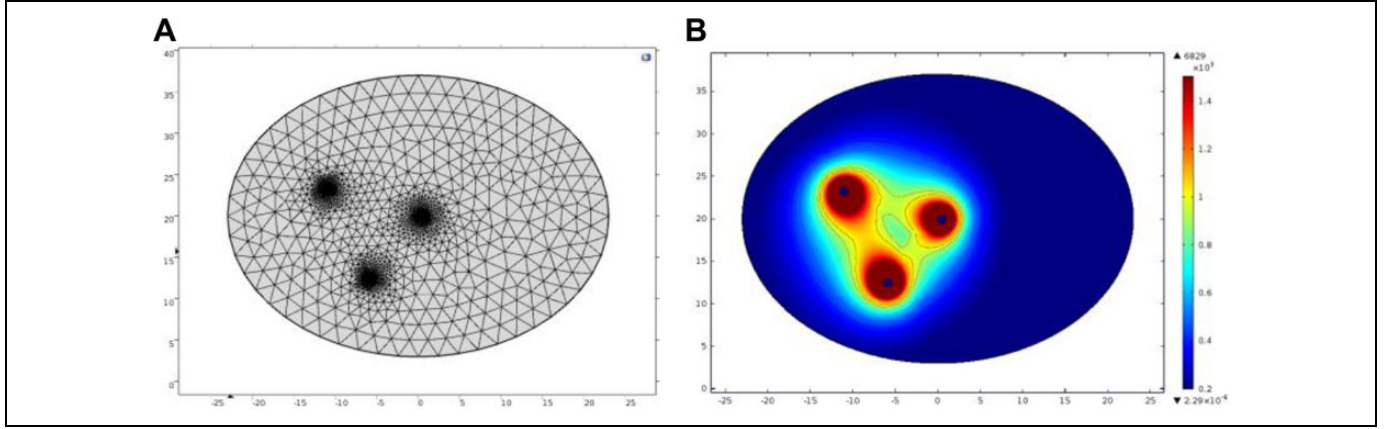


**Figure 2.** Mesh model and simulation result with 3 electrodes. The coordinate unit is mm. The field intensity unit is V/cm. (A) Mesh model. (B) Electric field intensity simulation.

the ellipse represents the prostate and the 3 small circles represent the electrodes. The diameter of the needle electrode was set at 1 mm, and the electrode spacing was set according to the measured distance in the ultrasound image. The tumors were not considered in the model because the dielectric parameters of prostate cancer were not clear when HF bipolar pulses were applied.

The electric field distribution in the biological tissue was closely related to the electrical conductivity and permittivity. The electrical conductivity and permittivity changes during the process of electroporation, but the dynamic response of tissue to HF bipolar pulses has been poorly researched; thus, in this study, the static model was used for an initial analysis. The fundamental frequency of the burst in this study was 33.3 kHz, and the corresponding permittivity and conductivity of the prostate tissues, which could be found from the reference,<sup>22</sup> were 7162.9 and 0.43292 S/m, respectively.

The Laplace equation was used to solve the electric field distribution in the tissue region. Within the solution domain, the electric current module was used to solve the following equations:

$$\nabla \cdot J = Q \left[ \frac{A}{m^3} \right], \quad (1)$$

$$J = \left( \sigma + \varepsilon_0 \varepsilon_r \frac{\partial}{\partial t} \right) E \left[ \frac{A}{m^2} \right], \quad (2)$$

$$E = -\nabla U \left[ \frac{V}{m} \right], \quad (3)$$

where  $U$  is the electric potential,  $E$  is the electric field,  $J$  is the current density,  $Q$  is the current source,  $\sigma$  is the conductivity,  $\varepsilon_r$  is the relative permittivity, and  $\varepsilon_0$  is the permittivity of free space. The boundaries surrounding 1 electrode were assigned a constant electrical potential:

$$U = U[V]. \quad (4)$$

The boundaries of the other electrode were assigned as a relative ground:

$$U = 0[V]. \quad (5)$$

The remaining boundaries were defined as electrical insulation:

$$n \cdot J = 0 \left[ \frac{A}{m} \right], \quad (6)$$

where  $n$  is the normal vector to the surface and  $J$  is the electrical current density.

The electric field distribution with isocontours can be determined using COMSOL software through electric field simulation. The electric field lethality threshold can be determined preliminarily by comparing the calculated electric field intensity contours and the ablation zone in MRI section and finding the electric field intensity closest to the ablation boundary.

## Results

The number of electrodes used in this clinical trial was 2 to 6 as shown in Table 1. The treatment time for each patient was <45 minutes, and there were no abnormalities during the pulse delivery process. Physiological indexes were monitored during treatment (including heart rate, blood oxygen level, and respiration rate), and all were found to be within the normal range. Low-dose muscle relaxants were injected before treatment; hence, muscle contractions did not occur during treatment. This is important because any major movements performed by the patients could potentially damage the nearby structures owing to the movement of electrodes.

After treatment, the patients felt well and could move around after approximately 10 hours. All patients were discharged from the hospital on the next day, and none required further hospitalization.

After 4 weeks, lesions were clearly visible in MRI scans. As shown in Figure 3, the areas surrounded by the red curve, namely, the darker regions, are the ablation areas. The areas surrounded by the blue curves are the prostate. In some cases, the electrode needles were positioned very close to the prostate capsule, but MRI scans revealed that the HF bipolar pulses had

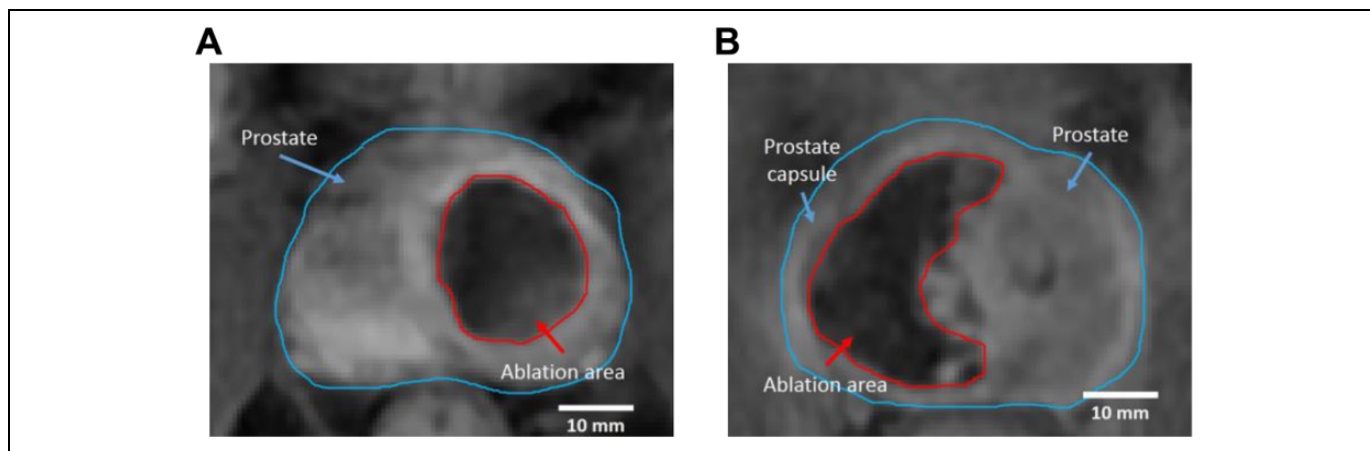


**Figure 3.** In MRI scans, lesions were clearly visible and the prostate capsule was noted to be intact. The area surrounded by the red curve is the ablation area, and the area surrounded by the blue curve is the prostate. (A) MRI of one patient before the treatment. (B) MRI of another patient before the treatment. MRI indicates magnetic resonance imaging.

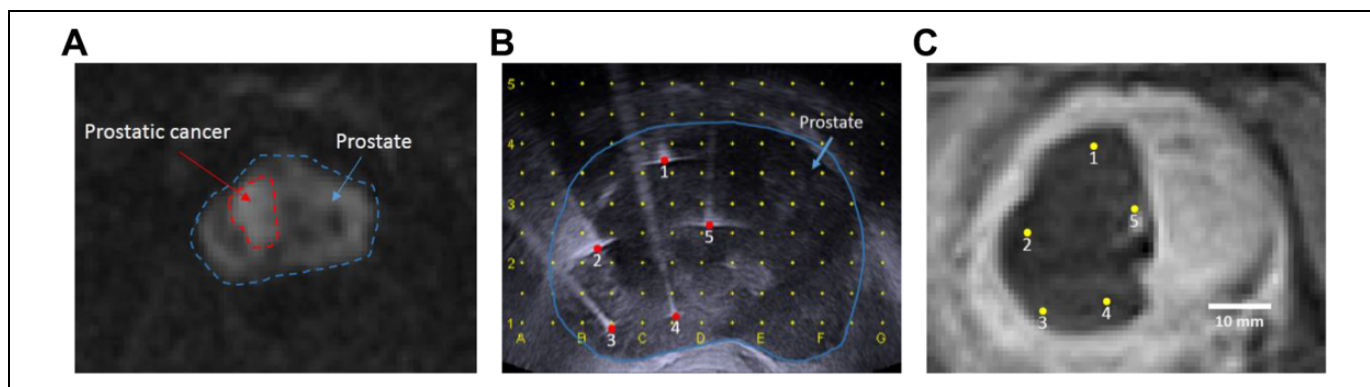


**Figure 4.** The electrode positions on the ultrasound images and MRI scans. The dots are the position of electrodes, and the area surrounded by the red dashes is the prostate cancer. The areas surrounded by blue dashes or blue curves are the prostate, and the dots are the position of electrodes. (A) MRI before the treatment. (B) Ultrasound image. (C) MRI after the treatment. MRI indicates magnetic resonance imaging.

not damaged the prostate capsule. Figure 3B also showed that the prostate capsule was intact, which could inhibit the metastasis of prostate cancer cells.

The location of prostate cancer was determined using MRI prior to treatment (Figure 4A). The therapeutic electrodes were then punctured transperineally at the margin of the cancer lesion under transrectal ultrasound guidance (Figure 4B). Comparing MRIs with ultrasound images facilitated the determination of electrodes positions in MRI scans as shown in Figure 4C. The electrode needles are all positioned in the ablation area, and the tissue between the electrodes has been completely ablated. The shape of the ablation area is closely related to the position of electrodes.

After determining the position of electrodes in MRI scans, the contours of the electric field distributions between each pair of electrodes were drawn as shown in Figure 5. Comparing the ablation boundaries and electric field distribution allows the preliminary determination of the electric field lethality threshold in the case of constant conductivity, and the average lethality threshold of the treatment protocol used in this trial was  $522 \pm 74$  V/cm.

The prostates of 8 patients were excised and used for histological analysis 4 weeks after treatment. Histological examination showed that the ablated area had diffuse necrotic glandular tissue without any obvious viable tissue within the ablated zone (Figure 6A). Although Figure 6B showed that large vessels in the tissue were intact, some amount of bleeding was observed near the electrodes with the appearance of scattered blood cells in the tissue, which may have been caused by capillary damage. The ablated zone was demarcated well from the immediately adjacent unaffected prostate parenchyma and the transition zone between the necrotic glandular tissue in the ablation area and the adjacent normal glandular tissue was abrupt (Figure 6C). In addition, necrotic glandular tissue was noted adjacent to the urethra as shown in Figure 6D. However, the urethral structural integrity remained intact without evidence of necrosis within the submucosa, even when the urethra was subjected to direct ablation during the safety portion of the study.

Patients were followed up for 6 months; in summary, the overall outcomes of our clinical treatment of patients with prostate cancer were that 8 of 40 patients underwent radical

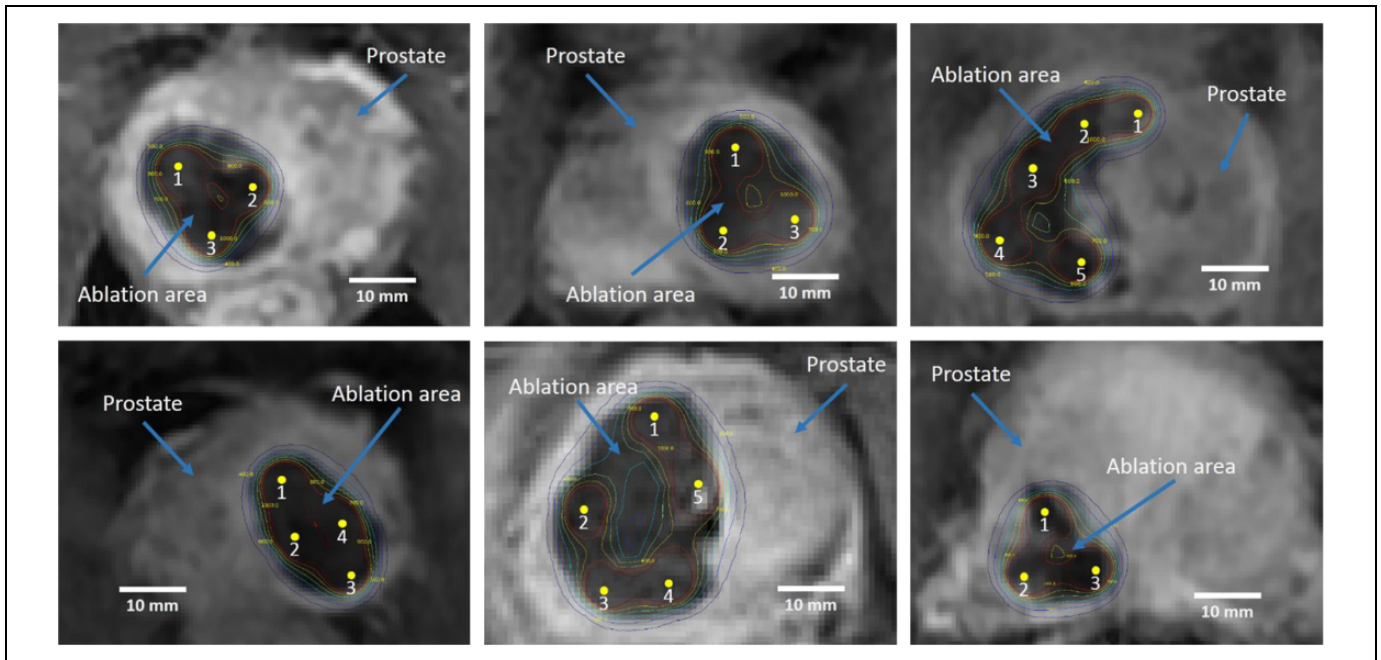


**Figure 5.** The electric field distribution contours in MRI. The color contours are the electric field intensity lines in the range of 400 to 1000 V/cm. The light gray area is the prostate and the dark gray area in the prostate is the ablation area. The yellow dots indicate the position of electrodes. MRI indicates magnetic resonance imaging.

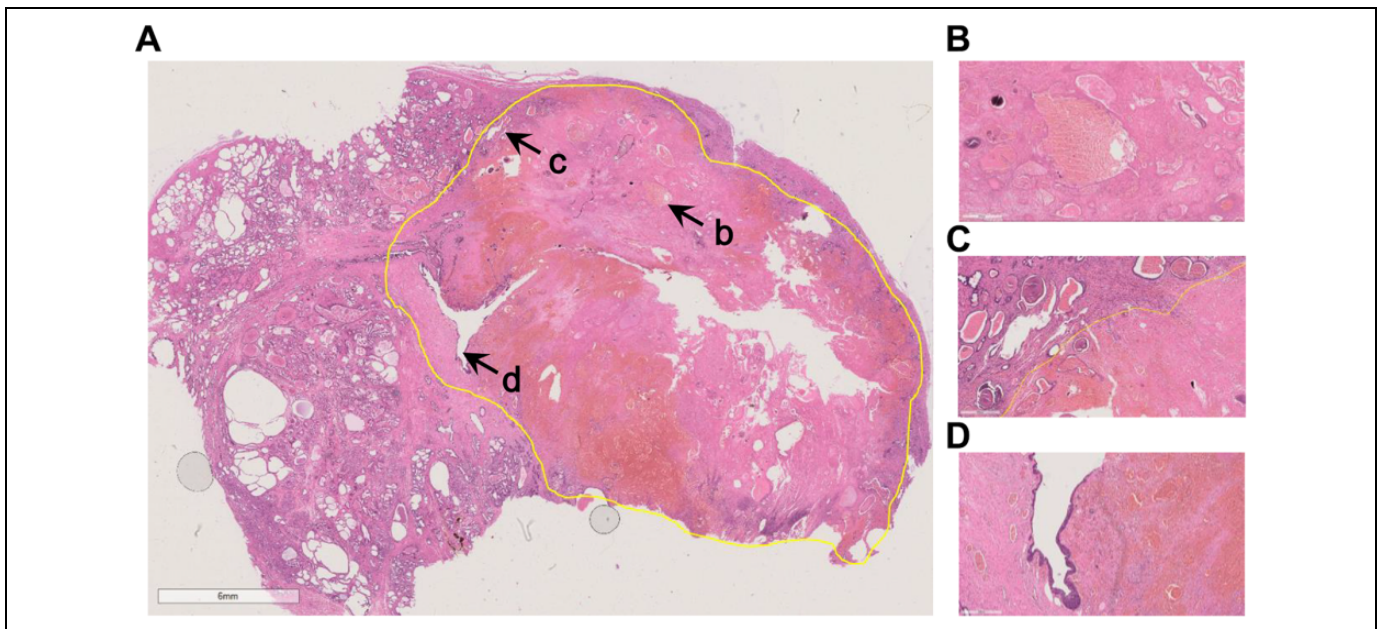


**Figure 6.** H&E stain of the prostate in which the ablation boundary is clear, there are no viable glandular tissues in the ablation area, and the urethra is intact after treatment. The yellow line is the ablation boundary. (A) H&E stain of prostate. (B) Larger vessels. (C) Ablation boundary. (D) Urethra. H&E indicates hematoxylin and eosin.

prostatectomy 4 weeks later, and 32 of 40 patients retained their prostates. Sexual function was preserved in 14 (100%) of 14 patients, 40 (100%) of 40 patients could control urination and did not require urinal pads, and 0 of 40 patients had urinary incontinence during surgery. The average hospitalization duration was 2 days, and the use time of urination was 2 to 10 days. Of the 40 patients, 15 (37.5%) presented hematuria 2 weeks

after surgery and 5 (12.5%) presented hematuria 4 weeks after treatment. None presented hematuria after 6 months.

## Discussion

Prostate cancer is one of the most common malignancies in older males. There are important blood vessels and NVB

around the prostate. A radical prostatectomy can cause severe trauma and impotence, while thermal ablation therapies can also injure adjacent structures, such as the rectum, urethra, and NVB, thereby causing some complications. Prostate cancer treatment needs to guarantee that tumor cells have been completely killed to prolong the patient survival. Moreover, it is preferable to preserve the function of the prostate because this will improve the quality of life.

Irreversible electroporation has several demonstrated advantages over well-known, thermal-based ablation methods. Many of these advantages stem from the mechanism of permanent destruction of the cell membrane, resulting in cell death in a nonthermal manner.

The first clinical trial of IRE for the treatment of prostate cancer published in 2010 showed good therapeutic effect.<sup>23</sup> However, during treatment, unipolar electric pulses can induce muscle contractions, unless deep muscle paralysis is maintained.

Arena *et al*<sup>18</sup> proposed a new type of pulse that utilizes an HF bipolar pulse burst to replace the traditional single monopolar pulse for tumor ablation. They also conducted ablation experiments on murine tumors to verify the effects of inhibition of muscle contraction and tumor growth.<sup>19</sup> Subsequently, Yao *et al*<sup>20</sup> systemically researched the ablation effect and muscle contractions by applying HF bipolar pulses to liver tissues *in vivo* and recommended 2 and 5 microseconds as the ideal width for individual pulses; this became an important parameter for clinical treatment. They also studied the difference between the dielectric property variations caused by traditional IRE pulses and HF bipolar pulses,<sup>24</sup> and pointed out that the HF bipolar pulse mitigates dielectric property variation to a higher extent than the conventional IRE pulses when fitting the dielectric spectrum data to the Cole–Cole model. In addition, Bhonsle *et al*<sup>25,26</sup> found that the area ablated by HF bipolar pulses is more consistent with the field distribution of the simulation, which helps doctors predict the ablation area. Siddiqui *et al*<sup>27</sup> carried out a series of experiments on pig liver, the results of which showed that increasing the number of bursts could improve the ablation area. Recently, Zhao *et al* showed the dynamic change in conductivity induced by HF bipolar pulses and compared it to conventional IRE.<sup>28</sup>

Ablation efficacy to a certain extent and muscle contraction outcomes were achieved in the present study using HF bipolar pulses with an individual pulse width of 5 microseconds, a total number of 250 bursts, and an applied voltage-to-distance ratio of 1500 V/cm. In addition, muscle paralysis was induced in HF bipolar pulse treatment to guarantee patient safety, but the muscle relaxant dosage was less than that used during traditional IRE.<sup>21,29</sup>

Here, the electric field threshold of ablation for HF bipolar pulses in human prostate cancer treatment was studied, and it was determined by comparing the electric field contours from simulation to the ablation area in MRI scans. The ultrasound imaging was recorded when the patients were placed in the dorsal lithotomy position, which is different from the position

of patients while undergoing an MRI. Therefore, there may be some errors in the determination of the electrode position by matching the ultrasound and MRI scans. In addition, the conductivity is set at a constant value, but during the treatment, the conductivity of the tissue will increase with the pulse applied, and the ablation area also changes<sup>30</sup>; hence, more accurate models that consider the dynamic conductivity should be built for multiparameter optimization in the future to predict the optimal ablation range.

Thermal ablation methods such as cryoablation,<sup>3</sup> radiofrequency ablation,<sup>31</sup> and microwave ablation,<sup>32</sup> have limitations caused by vessel heat-sink effect, which means that the tumors near the vessels cannot be completely ablated and thereby result in high local recurrence rates. In contrast, histological analysis demonstrated that lesions caused by HF bipolar pulses showed complete destruction, even extending to the vessel wall, without sparing the tissues adjacent to the vessel. Although an appearance of bleeding showed that the tissues had a capillary injury, the larger vessels in the tissues were intact. The preservation of the large vessels raises the possibility that there could be tissue regeneration in the ablated area.<sup>32,33</sup>

Preservation of the surrounding functional structures is very important during prostate cancer ablation. Although previous studies have demonstrated that urethra could be preserved without sloughing or major damage, some clinical cases showed that IRE has the potential to affect the urethra if it is located in the lethal electric field.<sup>34</sup> The pathological analysis conducted in this study revealed that the urethra remains intact, and this result may imply that HF bipolar pulses have advantages over IRE.

After treatment, the patients could recover quickly, and they were able to move about 10 hours after treatment without any uneasiness. The result that sexual function was preserved in 14 (100%) of 14 patients showed that the NVB was preserved during treatment, which made the patients more willing to accept this therapy.

## Conclusion

This study describes the first trial conducted in humans involving administration of HF bipolar pulses therapy for prostate cancer; HF bipolar pulse is a minimally invasive nonthermal therapy in tumor ablation that can reduce the dose of muscle relaxant during treatment. Compared to radical prostatectomy and thermal therapy, it can preserve the NVB, urethra, and major vasculature in the prostate, which is beneficial to patient recovery. The postoperative effect of such a treatment on patients was very encouraging, that is, sexual function was preserved in 14 (100%) of 14 patients, 40 (100%) of 40 patients could control urination and did not require urinal pads, and 0 of 40 patients had urinary incontinence during surgery. The clinical trials were conducted successfully, and they provide valuable insights regarding the treatment of prostate cancer using HF bipolar pulses, which will promote the ablation of solid tumors by IRE.

## Authors' Note

S.D., H.W., and C.Y. contributed equally to this work. Shanghai Changhai Hospital Ethics Committee, Ethical approval NO.: CHEC2017-075. All patients consented to the clinical trial verbally.


## Declaration of Conflicting Interests

The author(s) declared no potential conflicts of interest with respect to the research, authorship, and/or publication of this article.

## Funding

The author(s) disclosed receipt of the following financial support for the research, authorship, and/or publication of this article: This work was supported in part by the Natural Science Foundation Project of CQ CSTC (cstc2014jcyj00001), the Graduate Scientific Research and Innovation Foundation of Chongqing (CYB17011), the Fundamental Research Funds for the Central Universities (106112017CDJZRPY0103, 106112017CDJQJ158835), Key Industrial Generic Technology Innovation Special Project of CQ CSTC (cstc2015zdcy-ztzzX0003), and the National Natural Science Foundation of China (51321063).

## ORCID iD

Chenguo Yao, PhD  <http://orcid.org/0000-0002-1781-2756>

## References

- Chen W, Zheng R, Baade PD, et al. Cancer statistics in China, 2015. *CA Cancer J Clin*. 2016;66(2):115-132.
- Pound CR, Partin AW, Eisenberger MA, et al. Natural history of progression after PSA elevation following radical prostatectomy. *JAMA*. 1999;28(1):1591-1597.
- Hale Z, Miyake M, Palacios DA, Rosser CJ. Focal cryosurgical ablation of the prostate: a single institute's perspective. *BMC Urol*. 2013;13:1-6.
- Minami Y, Kudo M, Kawasaki T, et al. Percutaneous ultrasound-guided radiofrequency ablation with artificial pleural effusion for hepatocellular carcinoma in the hepatic dome. *J Gastroenterol*. 2003;38(11):1066-1070.
- Lau WY, Lai EC. The current role of radiofrequency ablation in the management of hepatocellular carcinoma: a systematic review. *Ann Surg*. 2009;249(1):20-25.
- Davalos RV, Mir IL, Rubinsky B. Tissue ablation with irreversible electroporation. *Ann Biomed Eng*. 2005;33(2):223-231.
- Yao C, Sun C, Mi Y, Xiong L. Experimental studies on Killing and inhibiting effects of steep pulsed electric field (SPEF) to target cancer cell and solid tumor. *IEEE Trans Plasma Sci*. 2004;32(4):1626-1633.
- Rubinsky B. Irreversible electroporation in medicine. *Technol Cancer Res Treat*. 2007;6(4):255-260.
- Maor E, Ivorra A, Rubinsky B. Non thermal irreversible electroporation: novel technology for vascular smooth muscle cells ablation. *PLoS One*. 2009;4(3):e4757.
- Rossmel JH, Jr, Garcia PA, Pancotto TE, et al. Safety and feasibility of the NanoKnife system for irreversible electroporation ablative treatment of canine spontaneous intracranial gliomas. *J Neurosurg*. 2015;123(4):1008-1025.
- Bos WVD, Bruin DMD, Muller BG, et al. The safety and efficacy of irreversible electroporation for the ablation of prostate cancer: a multicentre prospective human in vivo pilot study protocol. *BMJ Open*. 2014;4(10):e6382.
- Olweny EO, Kapur P, Tan YK, Park SK, Adibi M, Cadeddu JA. Irreversible electroporation: evaluation of nonthermal and thermal ablative capabilities in the porcine kidney. *Urology*. 2013;81(3):679-684.
- Wendler JJ, Pech M, Blaschke S, et al. Angiography in the isolated perfused kidney: radiological evaluation of vascular protection in tissue ablation by nonthermal irreversible electroporation. *Cardiovasc Intervent Radiol*. 2012;35(2):383-390.
- Dunki-Jacobs EM, Philips P, Martin RC II. Evaluation of resistance as a measure of successful tumor ablation during irreversible electroporation of the pancreas. *J Am Coll Surg*. 2014;218(2):179-187.
- Bertacchini C, Margotti PM, Bergamini E, Ronchetti M, Cadossi R. *Irreversible Electroporation Systems for Clinical Use*. Berlin, Germany: Springer; 2010:255-272.
- Zager Y, Kain D, Landa N, Leor J, Maor E. Optimization of irreversible electroporation protocols for in-vivo myocardial decellularization. *PLoS One*. 2016;11(11):e165475.
- Yao C, Zhao Y, Chengxiang LI, Yan MI, Liao R. Recent advances in tissue minimally invasive ablation with irreversible electroporation. *High Volt Eng*. 2014;40:3725-3737.
- Arena CB, Sano MB, Rossmel JH, et al. High-frequency irreversible electroporation (H-FIRE) for non-thermal ablation without muscle contraction. *Biomed Eng Online*. 2011;10:9144-9153.
- Sano MB, Arena CB, Bittleman KR, et al. Bursts of bipolar microsecond pulses inhibit tumor growth. *Sci Rep*. 2015;5:14999.
- Yao C, Dong S, Zhao Y, et al. Bipolar microsecond pulses and insulated needle electrodes for reducing muscle contractions during irreversible electroporation. *IEEE Trans Biomed Eng*. 2017;64(12):2924-2937.
- ChemicalBook. *Cisatracurium Besylate Basic information*. 2017. [http://www.chemicalbook.com/ProductChemicalProperties/CB7855410\\_EN.htm](http://www.chemicalbook.com/ProductChemicalProperties/CB7855410_EN.htm). Accessed December 20, 2017.
- Italian National Research Council. *Dielectric Properties of Body Tissues*. 2018. <http://niremf.ifac.cnr.it/tissprop/>. Accessed January 5, 2018.
- Onik G, Rubinsky B. *Irreversible Electroporation: First Patient Experience Focal Therapy of Prostate Cancer*. Berlin, Germany: Springer; 2010:235-247.
- Yao C, Zhao Y, Liu H, Dong S, Lv Y, Ma J. Dielectric variations of potato induced by irreversible electroporation under different pulses based on the cole-cole model. *IEEE Trans Dielectr Electr Insul*. 2017;24(4):2225-2233.
- Bhonsle SP, Arena CB, Sweeney DC, Davalos RV. Mitigation of impedance changes due to electroporation therapy using bursts of high-frequency bipolar pulses. *Biomed Eng Online*. 2015;14(suppl 3):1-14.
- Ivey JW, Latouche EL, Sano MB, Rossmel JH, Davalos RV, Verbridge SS. Targeted cellular ablation based on the morphology of malignant cells. *Sci Rep*. 2015;5:17157.
- Siddiqui IA, Latouche EL, Dewitt MR, et al. Induction of rapid, reproducible hepatic ablations using next-generation, high frequency irreversible electroporation (H-FIRE) in vivo. *HPB (Oxford)*. 2016; 18(9):726-734.



28. Zhao Y, Bhonsle S, Dong S, et al. Characterization of conductivity changes during high-frequency irreversible electroporation for treatment planning. *IEEE Trans Biomed Eng.* 2017;99:1-1.
29. Cheung W, Kavnoudias H, Roberts S, Szkandera B, Kemp W, Thomson KR. Irreversible electroporation for unresectable hepatocellular carcinoma: initial experience and review of safety and outcomes. *Technol Cancer Res Treat.* 2013;12(3):233-241.
30. Campelo S, Valerio M, Ahmed HU, et al. An evaluation of irreversible electroporation thresholds in human prostate cancer and potential correlations to physiological measurements. *APL Bioeng.* 2017;1(1):16101.
31. Calkins H, Reynolds MR, Spector P, et al. Treatment of atrial fibrillation with antiarrhythmic drugs or radiofrequency ablation: two systematic literature reviews and meta-analyses. *Circ Arrhythm Electrophysiol.* 2009;2(4):349.
32. Simon CJ, Dupuy DE, Mayosmith WW. Microwave ablation: principles and applications. *Radiographics.* 2005;25(suppl 1):S69.
33. Onik G, Mikus P, Rubinsky B. Irreversible electroporation: implications for prostate ablation. *Technol Cancer Res Treat.* 2007;6(4):295.
34. Bos WVD, Bruin DMD, Jurhill RR, et al. The correlation between the electrode configuration and histopathology of irreversible electroporation ablations in prostate cancer patients. *World J Urol.* 2016;34(5):657-664.